ENERGY INDEPENDENCE IN OPTICAL TRANSITION RADIATION IMAGING

J. Wolfenden*, R. B. Fiorito, C. P. Welsch, University of Liverpool, Liverpool, UK

Abstract

The exploitation of optical transition radiation (OTR) in imaging-based diagnostics for charged particle beams is a well-established technique. Simulations of the expected OTR transverse beam profiles are therefore important in both the design of such imaging systems and the analysis of the data. Simulating OTR images is relatively straight-forward for low energy electron beams. However, in the near future electron machines will be using high-energy and low-emittance beams. Using such parameters can be challenging to simulate, and can be limiting in their account of practical factors, e.g. chromatic aberrations. In this work we show systematically that the use of low-energy parameters in high-energy OTR image simulations induces little deviation in the resulting transverse beam profiles. Simulations therefore become much easier to perform, and further analysis may be performed. This opens up exciting opportunities to perform simulations quicker and with reduced demands on the computation requirements. It will be shown in this contribution how this approach will enable enhanced ways to optimize OTR diagnostics.

INTRODUCTION

Transition radiation is a broadband source of electromagnetic radiation which is produced as a charged particle crosses a boundary between two materials with different dielectric constants [1]. The optical range of this spectrum is known as optical transition radiation (OTR). This OTR can be collected with an optical system and imaged. The OTR image produced from a bunch of charged particles is a convolution of the transverse beam profile and the OTR single particle function (SPF) [2]. The OTR SPF is the image of OTR produced by a single particle. The SPF is largely dependent upon the imaging system used to image the OTR [2], in this way it is analogous to a point spread function (PSF) [3] in traditional optics. This convolution provides a diagnostic method for low-emittance, low-dispersion beams with sub-micrometer transverse profiles [4]. Currently OTR profile measurements are fit to the expected transverse distribution. For most applications this is a more than adequate methodology. However with sub-micrometer transverse beam sizes, the OTR image cannot be directly related to the beam profile. If the transverse beam size is comparable in width to the OTR SPF, the beam distribution will no longer dominate the convolution, and the image will not accurately reproduce the beam distribution. Therefore, the beam size cannot be directly recovered.

It has been shown previously [4] that it is still possible to extract the transverse beam size in these scenarios. A

---

* joseph.wolfenden@cockcroft.ac.uk

ratio known as the visibility has been demonstrated to be proportional to the beam size. The visibility is the ratio of the center intensity value of the OTR image and its peak intensity. Previous work has used an empirical formula and a self-calibration technique to extract this value. Presented in this contribution is a method to accurately simulate the OTR SPF for any imaging system, whilst significantly reducing the computational and temporal requirements. This OTR SPF can then be used in combination with real optical effects and a transverse beam distribution to reproduce beam sizes produced in previous work, and possibly further.

ENERGY INDEPENDENCE IN OTR SPF

Simulations of the OTR SPF require the OTR source electric field distribution. For an ultra-relativistic electron the longitudinal electric field becomes flattened in the direction of propagation, and the remaining transverse fields can be described as a pseudo-photon disc [5], with a characteristic width of $\gamma\lambda/2\pi$ [6], where γ is the Lorentz factor and λ is the wavelength of the emitted radiation. This pseudo-photon disc then reflects off the screen and produces real photons [7]. This leads to direct analytic solution for the OTR SPF source fields [6],

$$E^S_{(x_S,y_S)} = \frac{e\alpha}{\pi v} \frac{(x_S, y_S)}{\sqrt{(x_S^2 + y_S^2)}} K_1(\alpha\sqrt{x_S^2 + y_S^2}), \qquad (1)$$

where $\alpha = k/\gamma$, k is the wavenumber, v is the particle velocity, $K_1(x)$ is the first-order modified Bessel function of the second kind, (x_S, y_S) are spatial co-ordinates on the source plane.
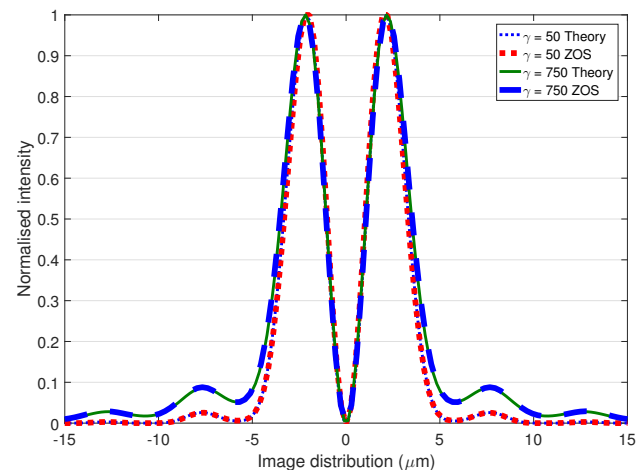
Figure 1: Comparison of OTR SPF simulation and theory from an ideal lens imaging system, at two beam energies.

06 Beam Instrumentation, Controls, Feedback, and Operational Aspects

T03 Beam Diagnostics and Instrumentation

Simulations are carried out using Zemax OpticStudio (ZOS) [8]. It can propagate transverse electric fields of any source through the surfaces of an imaging system. To ensure the accuracy of the ZOS simulations, the image field distribution produced using Equ. (1) was compared with that from theory. The electric field distribution found in the image plane of a single ideal lens [2] can be defined as,

$$E^i_{(x_i,y_i)} = \frac{2e}{\lambda M v} \frac{(x_i,y_i)}{\sqrt{x_i^2 + y_i^2}} \int_0^\infty \frac{\theta^2}{\theta^2 + \gamma^{-2}} J_1(\frac{k}{M}\sqrt{x_i^2 + y_i^2})d\theta,$$

(2)

where M is the magnification, θ is the viewing angle on the surface of the lens, $J_1(x)$ first-order Bessel function of the first kind, and (x_i, y_i) are spatial co-ordinates upon the image plane. The OTR SPF is then defined as [2],

$$P(x_i, y_i) = \frac{c}{4\pi^2}(|E^i_{x_i}|^2 + |E^i_{y_i}|^2).$$

(3)

The OTR SPF from a simple ideal lens system using ZOS was benchmarked against the image calculated using Equ. (3). Figure 1 proves ZOS can consistently reproduce the image distribution predicted by theory.

An OTR target must be larger than a few $\gamma\lambda/2\pi$ [9]. This is to ensure an infinite boundary can be assumed. This condition must also be upheld in simulations. This is the cause of a limting issue when simulating large γ beams. As the energy of the beam increases, so does the size of the source distribution. To maintain the required resolution across the source, the number of sampling points must also be increased. For example, to accurately simulate the OTR SPF produced by the 1.3GeV (γ = 2544) electron beam at the Accelerator Test Facility 2 (ATF2) (KEK, Japan), a sampling of 65,536 x 65,536 is required [9]. This leads to large requirements of both computational power and time, as the above parameters would require 350Gb of memory per surface propagation [8].
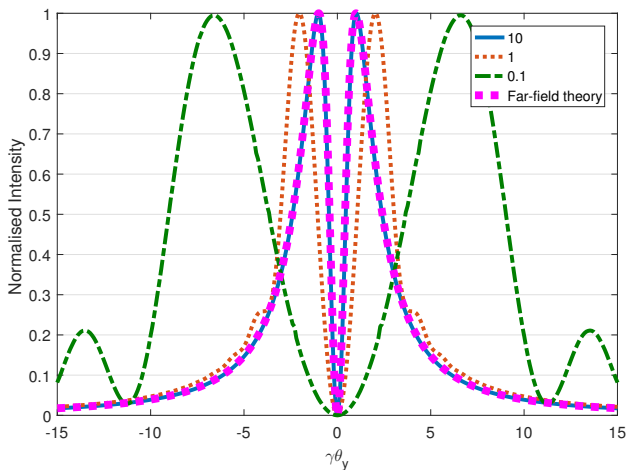
The angular distribution of OTR points indicates a possible method of reducing these stringent requirements. Figure 2 shows a comparison of the far-field angular distribution predicted by theory [10] and several angular distributions produced in ZOS for a range of distances. The distances are defined in terms of the formation length of the OTR, which is defined as $\gamma^2\lambda/2\pi$ [11]. This is used to define the far-field of an OTR source; i.e. a plane must be at a distance much greater than the formation length from the source to be treated as the far-field. Figure 2 shows the angular distribution from ZOS fits the theoretical far-field distribution at $10\gamma^2\lambda/2\pi$; it also matches results found previously via analytical methods [10].

In most applications an OTR imaging system cannot be placed at this distance, and is therefore placed in the near-field. Again from Fig. 2 it is clear that as the distance from the source increases, the distance between the intensity peaks decreases, until the well-known far-field result of $\theta_{peak} = 1/\gamma$ is found [10]. Therefore, as long as $\theta_m > 10/\gamma$, where θ_m is the angular acceptance of the imaging lens, the majority of the wavefront of the OTR distribution will be captured for most reasonable working distances. Logic ditates for a fixed angular field of view, if γ is increased to the point that $\theta_m > 10/\gamma$, then there would be no difference found in the resulting image distribution for larger γ. This argument has been shown previously mathematically [2], but to our knowledge the physical mechanism behind it has never been explored.

To demonstrate this concept Fig. 3 is a comparison of the OTR SPF, calculated using Equ. (3), from a high energy electron and a lower energy electron. It is evident that the differences between the two distributions are minimal overall; small discrepancies are found in the wings of the distribution but this is an area of little interest for beam size diagnostics. Reducing γ directly reduces the effective source size, which directly reduces the required simulation grid size and associated sampling; making the simulation process much quicker and more computationally efficient.

Figure 2: Comparison of OTR angular distributions from ZOS and theory. The different ZOS distributions are from different distances from the source in units of $\gamma^2\lambda/2\pi$, the formation length of OTR.
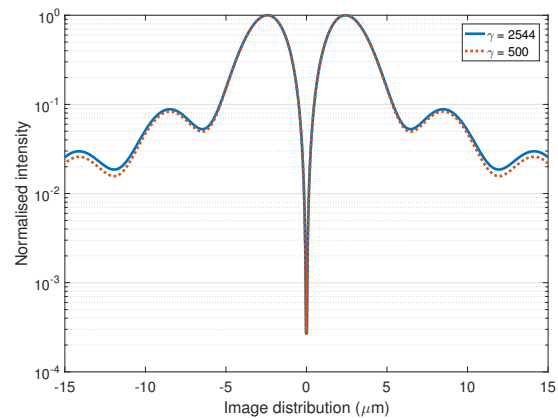
Figure 3: Comparison of the OTR SPF from an ideal lens imaging system, between 250 MeV and 1.3 GeV electrons.

06 Beam Instrumentation, Controls, Feedback, and Operational Aspects

T03 Beam Diagnostics and Instrumentation

ANALYSIS ALGORITHM

A novel analysis algorithm for OTR images of low-emittance electron beams has been designed implementing the simulation methodologies described above. A crucial component of this algorithm is the ability of ZOS to simulate real lenses. This means that optical systems can be directly reproduced for simulation purposes, including all the aberrations associated with the physical system.

Due to the increased simulation efficiency, more elaborate analysis is possible. One such analysis is the inclusion of chromatic aberrations created by using a bandwidth. This emulates the use on an interference filter, common practise in optical diagnostics. A convolution over wavelength can be carried out by performing the simulations repeatedly for a range of wavelengths spanning a bandwidth. As single wavelength results are often used, these chromatic effects are often missed. Figure 4 exemplifies why this effect is crucial to include in any OTR simulation.

Figure 4 is a comparison between the single wavelength result for a 3 μm transverse beam using a singlet lens (LA1050-A-ML, Thorlabs) and the same result with a 40 nm bandwidth. It is clear that the two distributions differ and would produce different visibility values; therefore different beam sizes. The difference in visibility will be dependent upon the bandwidth used. Without this analysis, when comparing single wavelength simulation results with data, the wrong beam size would be extracted from the image.
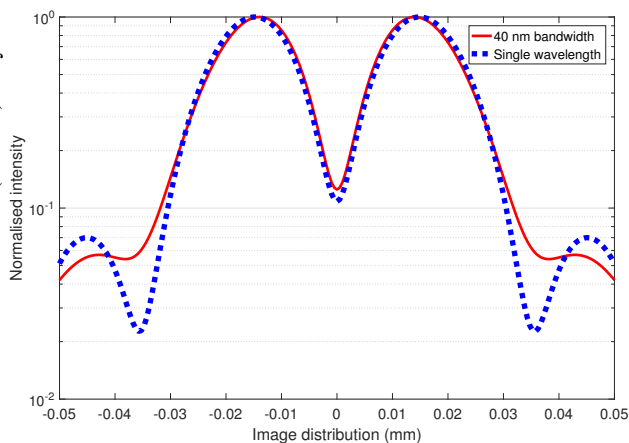
Figure 4: Comparison of ZOS results for single wavelength and bandwidth simulations of a 3 μm beam using a singlet.

The analysis algorithm is therefore a three-step process. The first is the definition of the source distribution. This is then propagated through an imaging system, producing an OTR SPF. This simulation can be carried out multiple times to calculate the influence of chromatic effects. Finally this chromatic OTR SPF is convolved with a transverse beam distribution.

DISCUSSION

The use of an innovative technique in simulating OTR SPFs has been demonstrated. Lower energy simulations can be used to reproduce higher energy results, only introducing negligible error in the resulting images. The combination of this methodology with a full optical system analysis algorithm provides a new process to retrieve transverse beam distributions from OTR images. This is especially pertinent for low-dispersion, low-emittance beams, where current profile fitting techniques would fail. Regardless of the limitations in certain parameter spaces, the possibilities provided by this algorithm are applicable to multiple areas of optical diagnostic research.

ACKNOWLEDGEMENT

REFERENCES

[1] M. L. Ter-Mikaelian, *High Energy Electromagentic Processes in Condensed Media* (Wiley-Interscience, New York, 1972).

[2] D. Xiang and W. H. Huang, "Theoretical considerations on imaging of micron size electron beam with optical transition radiation," Nucl. Instrum. Methods. Phys. Res. A **570**, 357–364 (2007).

[3] E. Hecht, *Optics* (Addison Wesley, Reading, 1987), 2nd ed.

[4] K. Kruchinin, A. Aryshev, P. Karataev, B. Bolzon, T. Lefevre, S. Mazzoni, M. Shevelev, S. T. Boogert, L. J. Nevay, N. Terunuma, and J. Urakawa, "Sub-micrometer transverse beam size diagnostics using optical transition radiation," J. Phys. Conf. Ser. **517**, 012011 (2014).

[5] D. Karlovets and A. Potylitsyn, "Transition radiation in the pre-wave zone for an oblique incidence of a particle on the flat target," Nucl. Instrum. Methods. Phys. Res. B **266**, 3738–3743 (2008).

[6] G. Kube, "Imaging with Optical Transition Radiation , Transverse Beam Diagnostics for the XFEL," DESY MDI Reports, (2008).

[7] D. Xiang, W.-h. Huang, and Y.-z. Lin, "Imaging of high-energy electron beam profile with optical diffraction radiation," Phys. Rev. ST Accel. Beams **10**, 062801, 1–12 (2007).

[8] Radiant ZEMAX, *Zemax OpticStudio 16.5, User's Manual* (2017).

[9] B. Bolzon, A. Aryshev, T. Aumeyr, S. Boogert, P. Karataev, K. Kruchinin, T. Lefevre, S. Mazzoni, L. Nevay, M. Shevelev, N. Terunuma, J. Urakawa, and C. Welsch, "Very high resolution optical transition radiation imaging system: Comparison between simulation and experiment," Phys. Rev. ST Accel. Beams **18**, 082803 (2015).

[10] V. Verzilov, "Transition radiation in the pre-wave zone," Phys. Lett. A **273**, 135–140 (2000).

[11] V. Ginzburg and V. Tsytovich, "Several problems of the theory of transition radiation and transition scattering," Phys. Rep. **49**, 1–89 (1979).

06 Beam Instrumentation, Controls, Feedback, and Operational Aspects

T03 Beam Diagnostics and Instrumentation